



LAWRENCE
LIVERMORE
NATIONAL
LABORATORY

NeutronSTARS Detector Modeling Report

R. J. Casperson, J. T. Burke, S. Fisher, E.
McCleskey

January 12, 2015

Disclaimer

This document was prepared as an account of work sponsored by an agency of the United States government. Neither the United States government nor Lawrence Livermore National Security, LLC, nor any of their employees makes any warranty, expressed or implied, or assumes any legal liability or responsibility for the accuracy, completeness, or usefulness of any information, apparatus, product, or process disclosed, or represents that its use would not infringe privately owned rights. Reference herein to any specific commercial product, process, or service by trade name, trademark, manufacturer, or otherwise does not necessarily constitute or imply its endorsement, recommendation, or favoring by the United States government or Lawrence Livermore National Security, LLC. The views and opinions of authors expressed herein do not necessarily state or reflect those of the United States government or Lawrence Livermore National Security, LLC, and shall not be used for advertising or product endorsement purposes.

This work performed under the auspices of the U.S. Department of Energy by Lawrence Livermore National Laboratory under Contract DE-AC52-07NA27344.

NeutronSTARS Detector Modeling Report

R.J. Casperson, J. T. Burke, and S. Fisher
Lawrence Livermore National Laboratory

E. McCleskey
Texas A&M University

Introduction:

Directly measuring (n,2n) cross sections on short-lived actinides presents a number of experimental challenges: scattered beam can produce a neutron background in the detectors, fission produces a substantial neutron background, and making a target from a short-lived isotope can be extremely difficult. The surrogate reaction technique is an experimental method for measuring cross sections on short-lived isotopes [1], and it provides a unique solution for measuring (n,2n) cross sections which addresses all three of these concerns. This technique involves measuring a charged-particle reaction cross section, where the reaction populates the same compound nucleus as the reaction of interest.

As an example, directly measuring $^{241}\text{Pu}(n,2n)$ would require creating a thick target of the isotope, which only has a 14.3 year half-life. With the surrogate approach, a thin target of ^{242}Pu would be used, which has a half-life of 375,000 years. A convenient reaction for this example is (α,α') with a 55 MeV α -particle beam, and with this reaction, scattered beam should not produce a substantial neutron background. Fission will still create a neutron background, but the thin target allows for direction detection of most fission events, and the background can therefore be subtracted. A ratio will be taken between the surrogate reactions $^{241}\text{Pu}(\alpha,\alpha'2n)$ and $^{241}\text{Pu}(\alpha,\alpha'f)$, and by multiplying by the known $^{241}\text{Pu}(n,f)$ cross section, the $^{241}\text{Pu}(n,2n)$ cross section can to be deduced.

To perform these measurements, a silicon telescope array will be placed along a beam line at the Texas A&M University Cyclotron Institute, and will be surrounded by a large tank of Gadolinium-doped liquid scintillator, which will act as a neutron detector. The combined charge-particle and neutron-detector arrays will be called NeutronSTARS. In the analysis procedure for calculating the (n,2n) cross section, the neutron detection efficiency and time structure will play an important role. Due to the lack of availability of isotropic, mono-energetic neutron sources, modeling will be essential in establishing this efficiency and time structure.

The remainder of this report will describe the modeling technique and results needed to calibrate the NeutronSTARS array. As calibration data will be needed to constrain the model, additional modeling work will be done to incorporate this data.

NeutronSTARS detector system:

The NeutronSTARS detector system will include a silicon telescope array for detecting light ions, as well as additional silicon detectors for measuring fission. These detectors will be housed in an aluminum vacuum chamber, and a target wheel will be

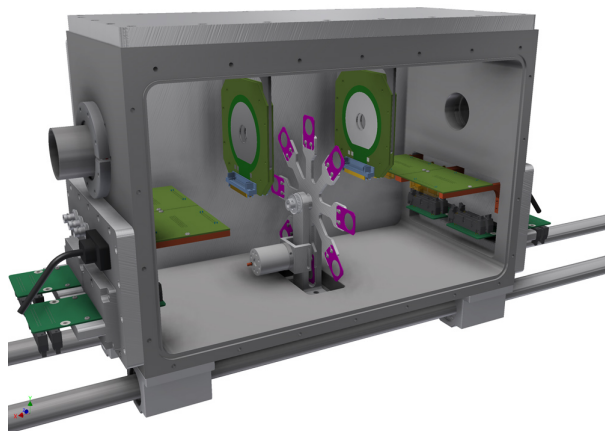


Fig. 1. A model of the NeutronSTARS vacuum system, illustrating vacuum components, electrical components, the target wheel, and the silicon detectors.

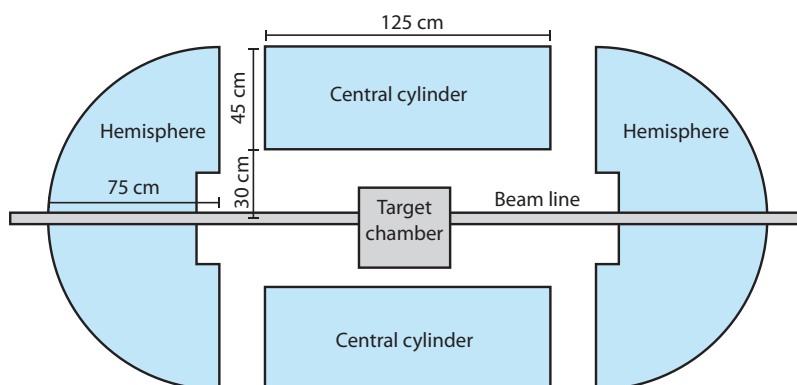


Fig. 2. A diagram of the Texas A&M Neutron Ball with the target chamber shown in the center.

positioned between the two sets of detectors. The design of the vacuum system can be seen in Fig. 1, with the silicon detectors separated for visibility.

The silicon telescope is positioned downstream of the target with regard to the beam direction. When an (α, α') event occurs in the target, energy is transferred to the target nucleus, and an α -particle of lower energy leaves the target. In the angle range of 30° to 60° the particle is detected by the silicon telescope, with some amount of energy deposited in a $150\ \mu\text{m}$ silicon detector, and the remainder deposited in a $1000\ \mu\text{m}$ silicon detector. The relative energy deposited in the two detectors can be used to identify the type of particle, and some other particles that can be produced include protons, deuterons, tritons, and ^3He . A thin layer of aluminum foil protects the silicon detectors to prevent electrons, α -particles and fission fragments from creating a large background in the telescope.

Upstream from the target are two $150\ \mu\text{m}$ silicon detectors, for detecting fission fragments. The first detector is positioned close to the target, and the second is set back, to ensure the maximum angular coverage for fission fragment detection. As each fission event produces two fission fragments, the array efficiency for detecting a fission event is twice the efficiency for detecting a fission fragment. There is very little energy dependence for

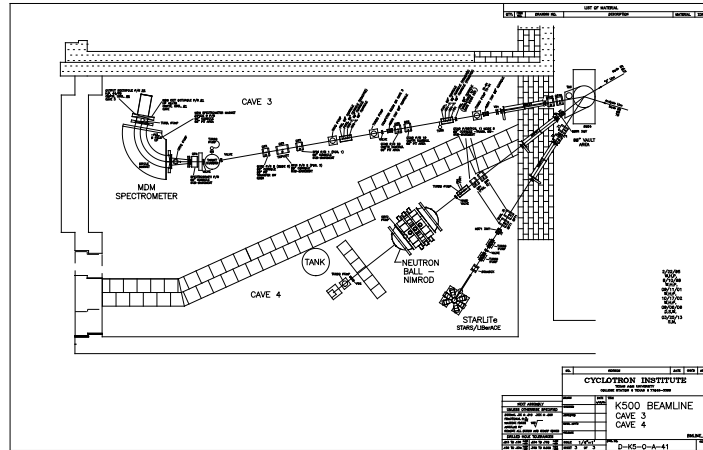


Fig. 3. Layout of Cave 4 at the Texas A&M Cyclotron Institute.

the detection efficiency of the fission detector, and the energy and efficiency can be calibrated in a straightforward manner using a ^{252}Cf source. The fission array efficiency is estimated to be about 60%.

The Texas A&M University Neutron Ball will be used as the neutron detection portion of NeutronSTARS, and has been used previously in experiments with the NIMROD charged particle array [2]. The array consists of six regions of Gadolinium-doped pseudocumene liquid scintillator, and the liquid scintillator has a total weight of about 3.5 tons. Fig. 2 illustrates the dimensions of Neutron Ball, and shows the relative position of the target chamber, which contains the silicon array. The central cylinder shown is divided into four wedges, and the wedges are separated by about 10 cm. This leaves gaps in the array, which allow neutrons to escape, but only decreases the detection efficiency by about 10%.

When a neutron enters Neutron Ball, it scatters off of the hydrogen in the liquid scintillator and quickly thermalizes. The cross section for $^{\text{nat}}\text{Gd}(n,\gamma)$ is very large at thermal energies, and the neutron quickly captures, producing a cascade of gamma rays. Liquid scintillator has a relatively long attenuation length for gamma rays, and the detector volume must be large to detect them. The gamma ray interactions in the liquid scintillator transfer energy to electrons, which interact with the liquid to produce scintillation light. The array efficiency for detecting neutrons does not have a straightforward estimate, as it can depend on the threshold energy cut, and neutron transport behavior. A monte carlo model can be used to identify the efficiency trend, and measurements can then be used to constrain the efficiency at specific energies.

Monte Carlo Modeling:

The software package Geant4 [3] was used for the monte carlo physics modeling of neutron interactions in the neutron detector. An existing simulation framework called GSim was previously written by the author to provide a reliable simulation design format for Geant4, as well as providing time-dependent output diagnostics for the visualization program GView.

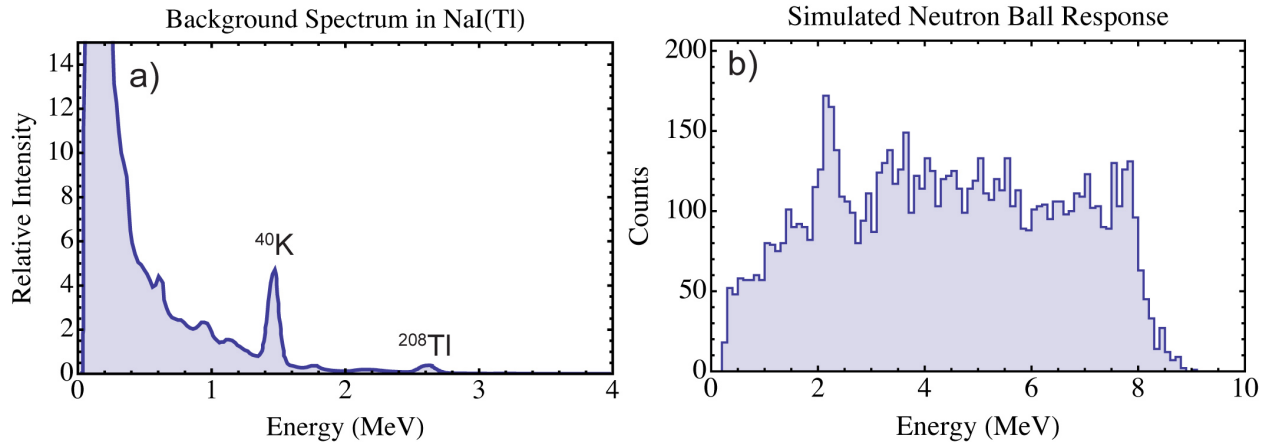


Fig. 4. a) Typical background spectrum in NaI(Tl) adapted from [4]. b) Detector response for 1 MeV neutrons simulated in Geant4.

The NeutronSTARS (n,2n) measurements will be performed in Cave 4 of the Texas A&M Cyclotron Institute. Fig. 3 shows the approximate layout of Cave 3 and Cave 4, which share a dividing wall, and Neutron Ball is shown on the right-hand side of the figure. The beam dump for the Neutron Ball beam line is not shown, and consists of a large block of concrete attached to the lower wall.

The detector arrays shown in Figs. 1 and 2 were modeled in a Geant4 simulation, and the geometry of the concrete shown in Fig. 3 was also added to the model. The Geant4 simulation used the QGSP_BERT_HP physics factory, with the Livermore electromagnetism physics class overriding the default electromagnetism class contained in the factory. An isotropic source of neutrons was produced at the target position, and the absorbed gamma energy distribution as a function of neutron energy was calculated.

Although the Neutron Ball geometry is large enough to produce a signal for most neutrons, not all gamma ray energy from $^{\text{nat}}\text{Gd}(n,\gamma)$ is absorbed by the detector. This is due to the long attenuation length of gamma rays in the liquid scintillator. If all measured energies are assumed to originate from neutrons, the neutron detection efficiency can be as high as 80% for 1 MeV neutrons. However, the liquid scintillator is responsive to background gamma rays, which could be misinterpreted as neutrons, and an energy threshold is needed to prevent this. Fig. 4a shows a typical NaI(Tl) detector background spectrum, illustrating the substantial background at low-energies, and the data shown is adapted from [4]. The 1.46 MeV gamma ray is from ^{40}K decay, and 2.61 MeV gamma ray is from ^{208}Tl decay, which is part of the ^{232}Th decay chain. Fig. 4b shows the Geant4 simulated detector response for 10,000 neutrons with 1 MeV of energy.

To eliminate backgrounds from ^{208}Tl decay, which originates from the ^{232}Th decay chain, an energy threshold can be placed on the measured detector energy. A cut of 2.8 MeV will remove most backgrounds, but will reduce the neutron detection efficiency by about 20%. A balance must be found to optimize detection efficiency, while reducing background events, and this balance can be found experimentally. The energy spectrum shown in Fig. 4b can be directly measured with a ^{252}Cf source at the target position, and the Neutron Ball background can be measured by recording data with no sources.

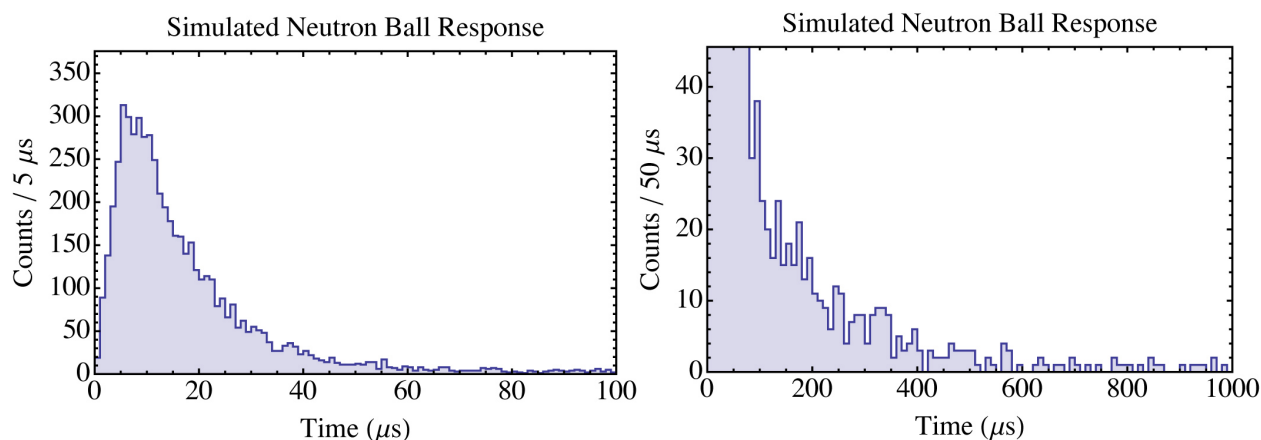


Fig. 5. Time response of Neutron Ball for 10,000 neutrons with 1 MeV of energy. The energy threshold was set to 2.8 MeV.

As the neutrons thermalize before capturing on Gd, there is a time delay between the $(\alpha, \alpha'2n)$ event and the detection of the neutron. This distribution can be calculated in Geant4, and the time spectrum for 1 MeV neutrons is shown in Fig. 5. There is a fast time component not shown, which would include gamma rays produced by the $(n,2n)$ event, as well as gamma rays produced by inelastic scattering of neutrons on the carbon in the liquid scintillator. This signal will not help in identifying the number of detected neutrons, and is ignored.

The long average thermalization time of the neutrons limits the event rate at which the experiment can be fielded, and this translates to lower beam current than those used in typical surrogate reaction experiments. Many of the late-time neutrons thermalize in the liquid scintillator, and escape back into the target chamber volume. At low energy, the flight across the central cavity can take hundreds of microseconds, which extends the time in which the system is busy. Modeling indicates that a 1 mm lining of Gd metal would dramatically reduce the number of neutrons detected at late times, and would in fact result in them being detected earlier. The sensitivity of the cross section to these delayed neutrons will need to be experimentally studied, before an upgrade to Neutron Ball is considered.

Detector Calibration:

In order to place an energy threshold on the neutron detector, a gamma energy calibration must be performed. Standard sets of gamma sources, including ^{137}Cs , ^{60}Co , and ^{228}Th will be used to determine the energy calibration. The neutron detector will measure gamma energies up to about 8 MeV, and finding calibration lines at this energy is difficult. The ^{228}Th source has a 2.6 MeV line that results from the decay of the daughter isotope ^{208}Tl , and this line can be seen in the NaI(Tl) background spectrum shown in Fig. 4a. Targets used in surrogate reaction experiments on actinides typically have a carbon backing, and a blank carbon target is used to isolate the effects of the carbon backing. Inelastic scattering on carbon (i.e., $^{12}\text{C}(\alpha, \alpha')$) frequently produces a 4.4 MeV gamma ray, which can also be used as a calibration line.

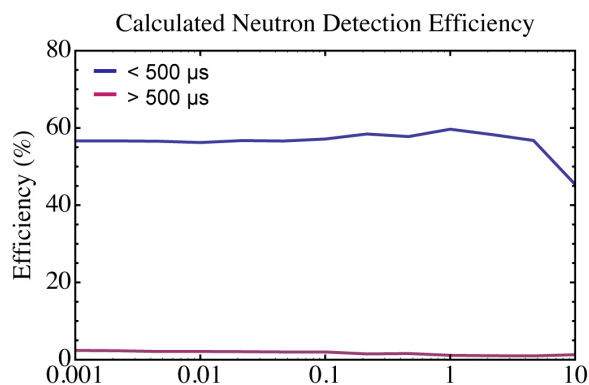


Fig. 6. Calculated neutron detection efficiency at early and late times. The energy threshold was set to 2.8 MeV.

After selecting an energy threshold for detecting a neutron, the array efficiency as a function of neutron energy can be calculated. The efficiency for detected neutrons that arrive before and after 500 μs can be seen in Fig. 6, which includes a 2.8 MeV energy threshold. Calibrating the efficiency of neutron detectors is challenging, as the desired source would be isotropic and mono-energetic, and such sources are not available. ^{252}Cf is a standard neutron-emitting source and the energy spectrum broad, but well understood. The overall amplitude of the detector efficiency can be constrained by multiplying the energy spectrum of the emitted neutrons with the calculated efficiency curve shown in Fig. 6. The energy distribution of the neutrons emitted from ^{252}Cf can be modified by surrounding the source with a layer of moderator, and this can be used as an additional calibration source.

Array Backgrounds:

The NaI(Tl) spectrum shown in Fig. 4a represents a typically energy spectrum in a gamma ray detector, and a similar spectrum is expected in Neutron Ball. The detector has an extremely large external surface area of about 13 m^2 , which will result in a large background gamma ray rate, but this quantity will need to be measured before an energy threshold is chosen. Any background gamma rays which are misidentified as neutrons will create a relatively constant rate of neutrons in the data. There is a procedure for subtracting background neutrons from the (n,2n) analysis, which will be described in the next section.

Fission is a major source of background neutrons, and these neutrons must be carefully taken into account during the analysis. Most fission events that occur with an α -beam incident on an actinide target involve fusion-fission, which has a much larger cross section than the $(\alpha, \alpha'2n)$ reactions of interest. These reactions produce a large number of neutrons and gamma rays, due to the 55 MeV of beam energy that is added to the compound nucleus, and should be identifiable even when a fission fragment is not detected. Events where a fission fragment is detected will allow for a characterization of this background in the neutron detector.

Other potential sources of neutrons include reactions in the beam dump or beam collimators, and these will be directly measured during the experimental campaign.

a) Probability matrix for 60% detection efficiency and 0 Hz background							b) Probability matrix for 60% detection efficiency and 2500 Hz background						
Number of produced neutrons	Number of detected neutrons						Number of produced neutrons	Number of detected neutrons					
	0	1	2	3	4	5		0	1	2	3	4	5
	0	1.0000	0	0	0	0		0	0.7408	0.2222	0.0333	0.0033	0.0003
	1	0.4000	0.6000	0	0	0		1	0.2963	0.5334	0.1467	0.0213	0.0021
	2	0.1600	0.4800	0.3600	0	0		2	0.1185	0.3912	0.3787	0.0965	0.0136
	3	0.0640	0.2880	0.4320	0.2160	0		3	0.0474	0.2276	0.3862	0.2658	0.0634
	4	0.0256	0.1536	0.3456	0.3456	0.1296		4	0.0190	0.1195	0.2910	0.3380	0.1849
	5	0.0102	0.0768	0.2304	0.3456	0.2592	0.0778	5	0.0076	0.0592	0.1881	0.3098	0.2768

Fig. 7. Probability matrices representing the number of neutrons detected when a specific number are produced, for a) 0 Hz background and b) 2500 Hz background.

Analysis Procedure:

The neutron detection efficiency shown in Fig. 6 is relatively flat over a large range of energies. Multiplying the measured efficiency by the expected neutron energy distribution allows for the determination of an overall detector efficiency for the reaction of interest. Using binomial statistics, a matrix can be formed representing the probabilities for the number of neutrons detected when a specific number of neutrons are produced, and such a matrix can be seen in Fig. 7a. When a constant neutron background is added, there is some probability of extra neutrons being measured in a given event. This probability can be represented by a Poisson distribution, and the resulting probability matrix is a convolution of a Poisson distribution with a binomial distribution. An example of this is shown in Fig. 7b.

Before the individual reaction channels can be isolated, the fission events must be subtracted from the data set. Most fission events can be identified by looking at fission fragment coincidences with the α -particle. Directly identifying $(\alpha, \alpha'f)$ events that do not have detected fission fragments is not possible, and the solution is to subtract the appropriately scaled fission neutron distribution from the neutron distribution for the rest of the data set.

As illustrated in Fig. 7, the number of emitted neutrons is not directly observed during an experiment, and must be determined from the distribution of detected neutrons. Spectra can be formed representing the number of detected neutrons, and by multiplying these spectra by the inverse of the probability matrix in Fig. 7, spectra of the individual reaction channels can be found. To find the $^{241}\text{Pu}(n,2n)$ cross section from the measured $^{241}\text{Pu}(\alpha, \alpha'2n)$ distribution, the last step is to multiply by the known $^{241}\text{Pu}(n,f)$ cross section, and divide by the measured $^{241}\text{Pu}(\alpha, \alpha'f)$ distribution.

Conclusions:

Directly measuring $(n,2n)$ cross sections on short-lived actinides is extremely difficult, and using an $(\alpha, \alpha'2n)$ surrogate reaction with the known (n,f) cross section is a promising solution to this problem. $^{241}\text{Pu}(\alpha, \alpha'2n)$ will be measured with the NeutronSTARS detector array, which includes a vacuum system with a silicon array, as well as a large Gd-doped liquid scintillator detector for neutron detection. Calibrating the neutron detector is challenging, and creating a monte carlo model of the array is an essential step in determining the neutron detection efficiency of the system.

A model has been developed in Geant4 to identify the energy and time response of NeutronSTARS, and to determine the neutron detection efficiency. The model will be constrained using a ^{252}Cf calibration source, potentially with a variety of moderation configurations. The appropriate energy threshold for neutron detection will be determined by measuring the $^{\text{nat}}\text{Gd}(n,\gamma)$ distribution in the detector, and by comparing it to the natural gamma-ray background of the system.

Neutrons that thermalize in the liquid scintillator and then travel back into the central cavity have a large potential for creating a delayed signal, which increases the chance of overlapping events. This may not have a significant impact on the cross section measurement, but a potential solution for the problem would involve lining the inner cavity with about 1 mm of Gd metal. This work performed under the auspices of the U.S. Department of Energy by Lawrence Livermore National Laboratory under Contract DE-AC52-07NA27344.

References:

- [1] J. E. Escher *et al.*, RMP **84**, 353 (2012).
- [2] R. P. Schmitt *et al.*, NIM A **354**, 487 (1995).
- [3] S. Agostinelli *et al.*, NIM A **506**, 250 (2003).
- [4] A. L. Mitchell, R. T. Kouzes, J. D. Borgardt, PNNL-18666, PNNL, 2009.